Eng. Fracture Mechanics, 73, 2006, 2304-2323

A CRITICAL INVESTIGATION OF THE USE OF A MANDREL PEEL METHOD FOR THE DETERMINATION OF ADHESIVE FRACTURE TOUGHNESS OF METAL-POLYMER LAMINATES

L F Kawashita, A J Kinloch, D R Moore, J G Williams
Imperial College London

ABSTRACT

The application of peel tests for the measurement of adhesive fracture toughness of metal-polymer laminates is reviewed and the merits of a mandrel peel method are highlighted. The mandrel method enables a direct experimental determination of both adhesive fracture toughness (G_A) and the plastic bending energy (G_P) during peel, whilst other approaches require a complex calculation for G_P. In this method, the peel arm is bent around a circular roller in order to develop a peel crack and an alignment load attempts to ensure that the peel arm conforms to the roller.
The conditions for peel arm conformance are thoroughly investigated and the theoretical basis for conformation are established. Experimental investigations involve the study of the roller size (radii in the range 5 mm to 20 mm are used), the peel arm thickness (varied from 0.635 mm to 2.0 mm) and the magnitude of the alignment load. In addition, the plane of fracture is studied since fractures can vary from cohesive to interfacial and this has a profound influence on the value of G_A and on interpretation of results.
A test protocol for conducting mandrel peel is developed such that the roller size for peel arm conformance can be established from preliminary fixed arm peel tests.
The work is conducted on two epoxy/aluminium alloy laminates suitable for aerospace applications. Comparative results of adhesive fracture toughness from mandrel peel and multi-angle fixed arm peel are made with cohesive fracture toughness from a tapered double cantilever beam test.

KEYWORDS
Adhesive fracture toughness, cohesive fracture toughness, fracture mechanics, peel tests, adhesive joint tests, interfacial fracture.

A CRITICAL INVESTIGATION OF THE USE OF A MANDREL PEEL METHOD FOR THE DETERMINATION OF ADHESIVE FRACTURE TOUGHNESS OF METAL-POLYMER LAMINATES

L F Kawashita, A J Kinloch, D R Moore, J G Williams
Imperial College London

INTRODUCTION

The use of polymeric adhesives for bonding metal structures is well established in aerospace and automotive applications. The performance of a metal-polymer system can be monitored through a number of fracture tests involving peel of a laminate or crack growth in a joint test [e.g.1-3]. Of course, numerous options are available for peel or adhesive joint tests. However, there is a growing recognition that geometry independent performance assessments of adhesive strength can be significantly more helpful and thus fracture mechanics methods are used for these occasions [4]. In this context, a global energy analysis has been adopted whereby the total energy associated with fracture is assigned to each of the contributory energy components (adhesive fracture energy, elastic deformational energy, plastic deformational energy, kinetic energy etc.) [5]. Such an approach has been successful for both peel and adhesive joint tests [3, 6].

The polymeric adhesive is only part of the bonded structure and often polymeric primers and other surface treatments are applied to the metal substrate during preparation. In addition, the choice and thickness of the substrate can be varied. From a fracture standpoint, this allows the possibility of a complex plane of fracture. Consequently, the fracture maybe cohesive in either a symmetric or an asymmetric sense, or it may also be interfacial [7]. Inevitably, such ramifications are the reality of bonded joint systems and therefore the assessment of performance should accommodate these variations. Peel tests accommodate these variables of fracture more naturally than adhesive joint tests, particularly for the tests based on fracture mechanics analysis where adhesive fracture toughness (G_A) is determined [8]. At the same time, this is a virtue for the adhesive joint tests based around the double cantilever beam geometry (tapered or straight) since they provide a clear measure of cohesive fracture toughness (G_C) [3,7].

There are a number of peel tests that may be used for assessing the performance of metal-polymer laminates. These include fixed arm, T-peel and roller assisted peel tests such as climbing drum, floating roller and mandrel peel. Moreover, a global energy analysis has been conducted for each test enabling adhesive fracture toughness to be determined [8-10]:

$$G_A = G - G_P(R_0) \qquad (1)$$

where G is the total external energy used for peel fracture and $G_P\ (R_0)$ is the plastic bending energy associated with deforming the peel arm to a minimum radius of curvature R_0.

In the determination of adhesive fracture toughness from most peel tests, it is necessary to measure peel strength (peel force per unit width, P/b) in order to obtain G, and then to calculate G_P using available software known as *ICPeel* [11]. The calculation of G_P requires a measurement of the tensile stress-strain behaviour of the

peel arm material, which must then be then fitted to a specific mathematical function (a bilinear or linear-power law) [9]. Although the *ICPeel* software provides a ready means for conducting the calculations, there are a number of intricacies and possible sources of error in the procedure [12]. A mandrel peel method does not require this approach because both G_A and G_P can be obtained directly by experiment [8, 13, 14, 15]. Consequently, this method offers an approach that eliminates some of the complications in other peel methods.

In the mandrel peel test, peel fracture is achieved by fixing one adherend of the laminate onto a low friction trolley whilst passing the other adherend (the peel arm) around a friction-free roller prior to peeling. The feature that differentiates the mandrel peel method from other roller assisted methods is that the base trolley has an applied alignment load that can be adjusted in order for the peel arm to conform to the mandrel roller. In addition, the radius of the roller can be selected from a wide range in order to establish suitable experimental condition (as will be discussed later). Full details of our equipment are given in the references [8, 15], although some details are also given in the section on Experimental Methods.

Previous work with a mandrel procedure has demonstrated the concepts and theory associated with the method [8, 13, 14, 15]. The purpose of the current work is to investigate all aspects of the use of the procedure for metal-polymer laminates. In particular, it is intended to explore the size of the mandrel roller, the role and magnitude of alignment load and the influence of specimen variables such as peel arm thickness.

The work will use the mandrel technique in order to determine adhesive fracture toughness, but in addition, the same laminates will be tested using a fixed arm peel method. The fixed arm test will enable the adhesive fracture toughness to be obtained by an independent approach but will also enable the calculation of peel arm curvature (R_0) [12] by using *ICPeel* software [11]. Consequently, it is intended to rigorously investigate the criteria for conformance of the peel arm to the mandrel roller and hence establish a formal experimental protocol for the mandrel method.

MATERIALS AND EXPERIMENTAL METHODS

Materials

Two epoxy adhesives were used in this work, FM73 (supplied by Cytec Engineered Materials) and the other designated adhesive F. Both adhesives are industrial products intended for high performance applications such as aerospace. FM73 is a commercial grade whilst adhesive F is an experimental compound whose exact formulation is not known, however, it is understood that both formulations are based on Bisphenol-A epoxy resins with a rubber toughening agent. They were in the form of film adhesives and therefore had a polymer fabric to give them support in the uncured state.

The laminates for both epoxy adhesives were bonded as 230 mm x 350 mm sheets with an unbonded portion (about 55 mm) in the long side. The sheet was a sandwich of 2024-T3 aluminium alloy (AA) with epoxy compound at the centre. Thickness of the top plates was 0.63 mm, 1.63 mm or 2.0 mm, whilst the bottom plate was 1.63 mm or 2.0 mm thick. Both AA substrates were treated in a FPL etching process and sprayed with an epoxy-based primer compound (BR127). The primed AA plates were cured for 120 minutes at 133^{o}C in an autoclave under pressure. Both gave a bond-line thickness of about 120 μm.

Parallel strips were cut and subsequently machined to produce a specimen with peel arm widths of 15 mm (for all thickness of peel arms) and 10 mm (for 1.63 mm or 2.0 mm thick peel arms) and a base plate in width of 30 mm that could be bolted to the mandrel peel table. Both mandrel peel and fixed arm peel tests could be conducted with this specimen.

Mandrel peel and fixed arm tests

The mandrel peel equipment is shown in Figure 1 whilst others details are given in reference [8] and [15]. The base of the laminate is attached to a table that is positioned on a linear bearing system that minimises friction during the peeling process. The peel arm is bent around a circular roller (the mandrel) whilst an alignment force is applied to the base of the laminate. The roller incorporates ball bearings to further reduce frictional effects. Mandrel radii were available in the range 5 mm to 20 mm. The peeling strip was attached to an Instron testing machine and peel force (*P*) was monitored as a function of alignment force (*D*).

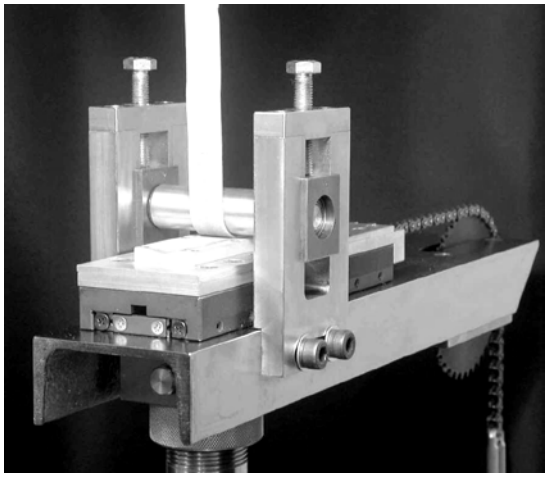

Figure 1 The mandrel peel apparatus.

Analysis of the mandrel procedure [8] can be shown with reference to the schematic of Figure 2

For low friction, equating the moments around the axis gives $F=P$ and then by equating horizontal forces, the alignment force is given by:

$$D = P(\cos\theta + \cos\theta_1) \tag{2}$$

The general peel equation [6] defines G:

$$G = \frac{P}{b}(1 - \cos\theta) \tag{3}$$

For our equipment, θ_1 is 90^o therefore

$$G = G_A + G_P = (\frac{P}{b} - \frac{D}{b}) \tag{4}$$

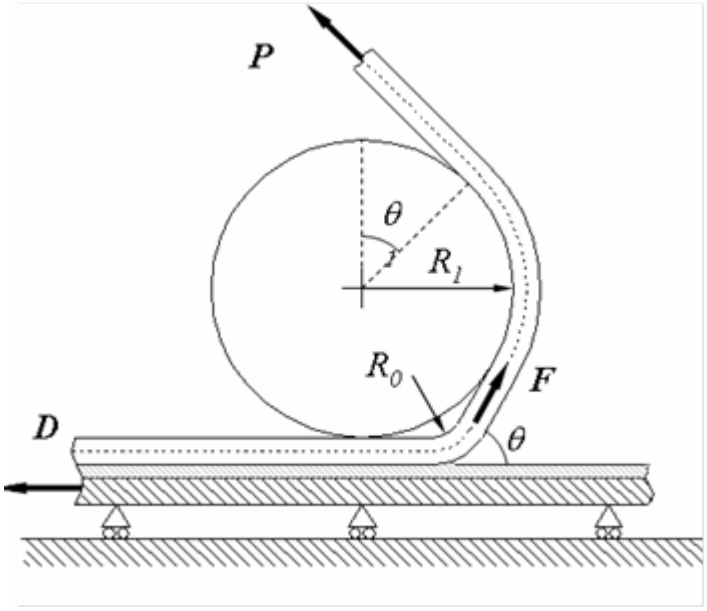

Figure 2 Forces in our mandrel peel test.

Consequently, the mandrel procedure, with a roller of radius R_1, will involve two tests. First, with an unbonded specimen where $G_A = 0$ and second with a bonded specimen where G_A is the adhesive fracture toughness. Results are presented as plots of P/b versus D/b as shown schematically in Figure 3.

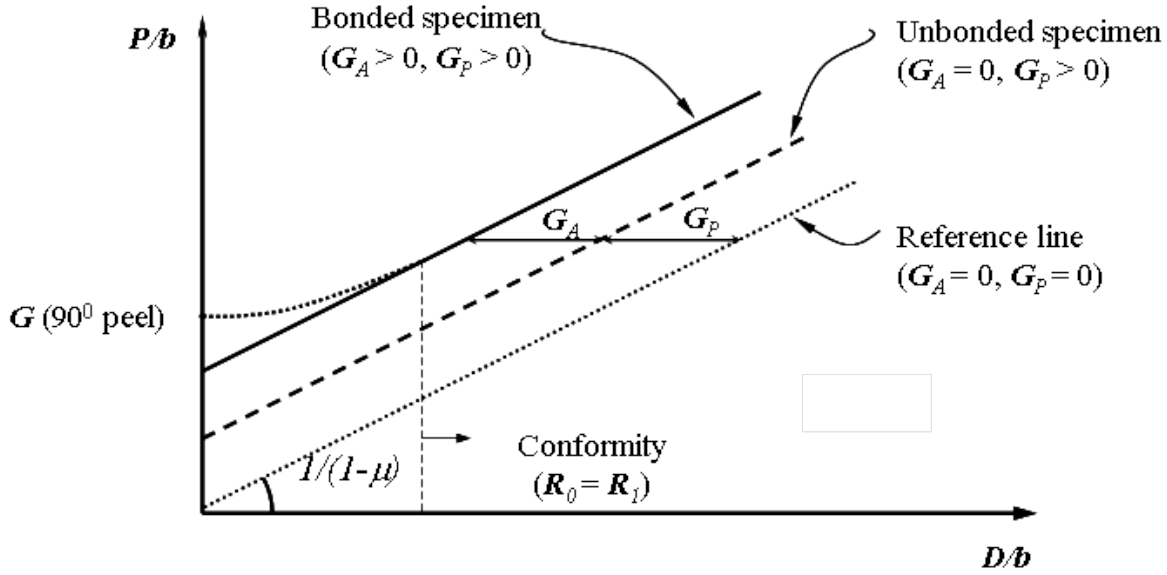

Figure 3 Schematic of results from a mandrel peel test procedure.

The mandrel test, described here, is designed to be versatile in that D is applied independently and so θ changes (see Figure 2), hence R_0 changes and conformity can be achieved. For an unbonded specimen R_0 is large and conformity is guaranteed and data in the form of P_0/b versus D_0/b is shown in Figure 3 with a slope of unity (for zero friction) but displaced by $G_P(R_1)$ as shown.
For the bonded specimen at $D = 0$, $\theta = 90^o$ so the value is as in the 90^o peel test and usually $R_0 < R_1$ and $P/b > G_P(R_0) + G_A > G_P(R_1) + G_A$. As D increases θ decreases and so R_0 increases until $R_0 = R_1$ and conformity occurs as shown in Figure 3. For larger D values the lines should be parallel and displaced by G_A.
Generally the friction is low in such tests (coefficient of friction μ < 2%) [15], but it can be calibrated out as shown in Figure 3.
An alternative way of presenting results is in the form of plots of G_A versus D/b where individual data are used to determine G_A [15]. This will be used extensively in this work.
The fixed arm peel tests were conducted at peel angles of 45^o, 90^o and 135^o for the laminate based on adhesive F and just at 90^o for the laminate based on FM73. A variable angle fixed arm apparatus was used that accorded to the European Structural Integrity Society (ESIS) test protocol [10]. The mandrel equipment was used for this test but with the roller removed. This achieved a 90^o fixed arm peel. A 45^o wedge was then attached to the mandrel table in order to obtain a 45^o fixed arm set-up and by reversing the wedge, a 135^o fixed arm set-up. Data analysis is done using *ICPeel* software [11]. When mandrel data are compared with fixed arm results, it is the average of all fixed arm data that are used, unless only 90^o fixed arm results were available (as in the case of FM73/AA2024 T3).
In all cases (mandrel and fixed arm peel) the crosshead speed was adjusted in order to give a constant 5mm/min peel crack growth, and tests were performed at standard air conditions (21^0C, 55% RH). Peel data were collected over lengths of at least 50 mm.

Tensile stress-strain.
Tensile stress-strain measurements were conducted on the peel arm material in order to provide a necessary input to the calculations of plastic bending energy using *ICPeel* and the ESIS protocol [10]. Parallel strip specimens were tested at 1 mm/min (strain rate of 2×10^{-3}) where an optical extensometer was used to measure axial strain. A bilinear function was fitted to the stress-strain results in order to comply with the requirements of data analysis [9] and although the ESIS test protocol [10] describes how this should be achieved it is perhaps helpful to indicate that the yield co-ordinates must be identified first before fitting the linear plastic curve.

Cohesive fracture toughness
Cohesive fracture toughness (G_C) was measured using tapered double cantilever beam geometry (TDCB). For Adhesive F, test details and results are given in reference [7] and a symmetric cohesive fracture was obtained. The same procedure was used for FM73 and results are summarised in a later section; a symmetric cohesive fracture was obtained.

RESULTS AND DISCUSSION

Preamble
Two sets of results will be presented; one from mandrel peel tests and the other from fixed arm peel tests. In both cases the peel arm will be inspected in order to establish

the plane of fracture i.e. whether there is visible adhesive on the peel arm (cohesive fracture) or whether there is so little adhesive visible with a naked eye, that the plane of fracture can be described as interfacial.

The fixed arm peel results will provide a value for G_A and since this is derived from equation 1 using *ICPeel*, it will also be possible to calculate the radius of curvature of the peel arm (R_0). The mandrel test uses a 90^o angle between alignment force and peel force, therefore the radius of curvature associated with a 90^o fixed arm test peel will be used for comparison with the roller radius in the mandrel test, in order to make a judgment as to whether the peel arm is conforming to the roller in the mandrel test.

The mandrel results will provide plots of G_A versus *D/b* and the size of roller radius and peel arm thickness will be varied. The aim in examining the mandrel data will be to establish whether the peel arm is conforming to the mandrel or not and whether the results are cohesive, interfacial or transitional (e.g. starting cohesive and becoming interfacial [7]). Inevitably, there will be other features also requiring an explanation.

Results will be presented in three sections. First, for laminate AA2024 T3/FM73 with a peel arm of 0.635 mm and where only two mandrel radii were used. Second, for laminate AA2024 T3/Adhesive F with a peel arm of 0.635 mm but for a wider range of mandrel radii. Third for laminate AA2024 T3/Adhesive F with thicker peel arms (1.635 mm and 2.0 mm).

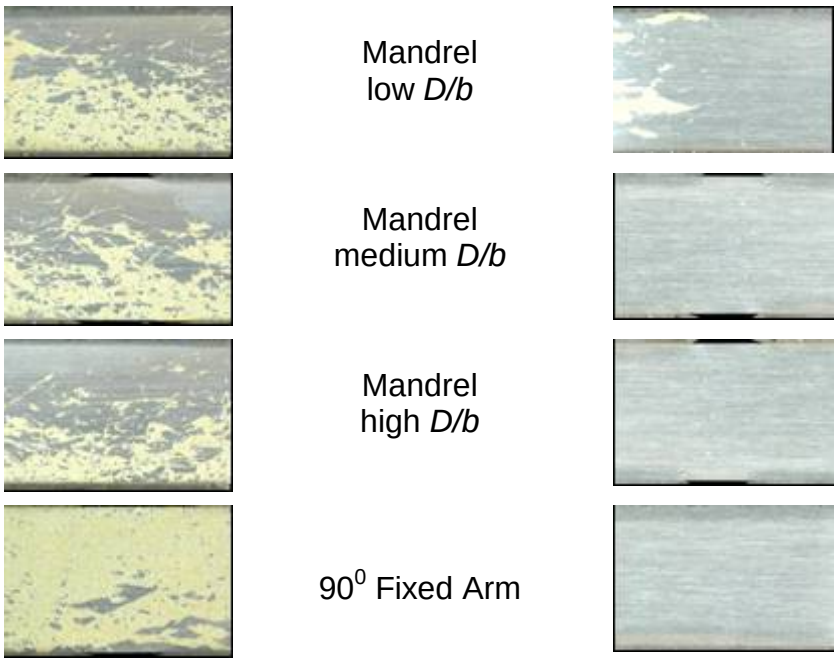

Figure 4 Photographs of peel arms of 0.635 mm AA 2024 T3/FM73 from fixed arm and mandrel peel (Specimen A1 on the left specimens A2/A3 on the right).

Results for 0.635mm AA2024 T3/FM73 laminate

Fixed arm peel measurements were conducted at one peel angle (90^o) with this laminate. Three specimens were tested in fixed arm peel and the same specimen was then used for mandrel peel without removing it from the peel instrument. Photographs of the peel arms for both fixed arm peel and mandrel peel are shown in Figure 4. Although adjacent specimens from the original plate were used, the plane of fracture

was cohesive for one specimen (numbered A1) but interfacial for the other two (numbered A2 and A3). Figure 4 shows the peel arms at three levels of alignment load (*D/b*). The small amount of adhesive coating on the left side of specimen A2 and A3 at low alignment load related to some cohesive fracture during setting up of the mandrel specimen and not during the actual peel cracking. Therefore, all aspects of fracture for these two specimens were entirely interfacial. Specimen A1 showed some interfacial fracture regions, but there was sufficient adhesive coating for the fracture to be considered as cohesive (albeit asymmetric in nature).

The 90^o fixed arm peel results on specimen A1 enable the radius of curvature of the peel arm (R_0) to be calculated from *ICPeel* and a value of 6.85 mm is obtained. Consequently, mandrel peel measurements with a 5 mm roller radius (R_1) should provide a condition where the peel arm conforms to the mandrel roller, since $R_0 > R_1$.
Peel results for specimen A1 are shown in Figure 5 and include fixed arm peel, mandrel peel and fracture toughness from TDCB test. For specimen A1, all peel data relate to asymmetric cohesive fracture and the TDCB results relate to symmetric cohesive fracture. G_A from the mandrel test is independent of alignment load implying that conformance to the roller is achieved at low alignment loads.
There is excellent agreement between the G_A values from mandrel and fixed arm peel and these agree with the value of G_C from the TDCB test.

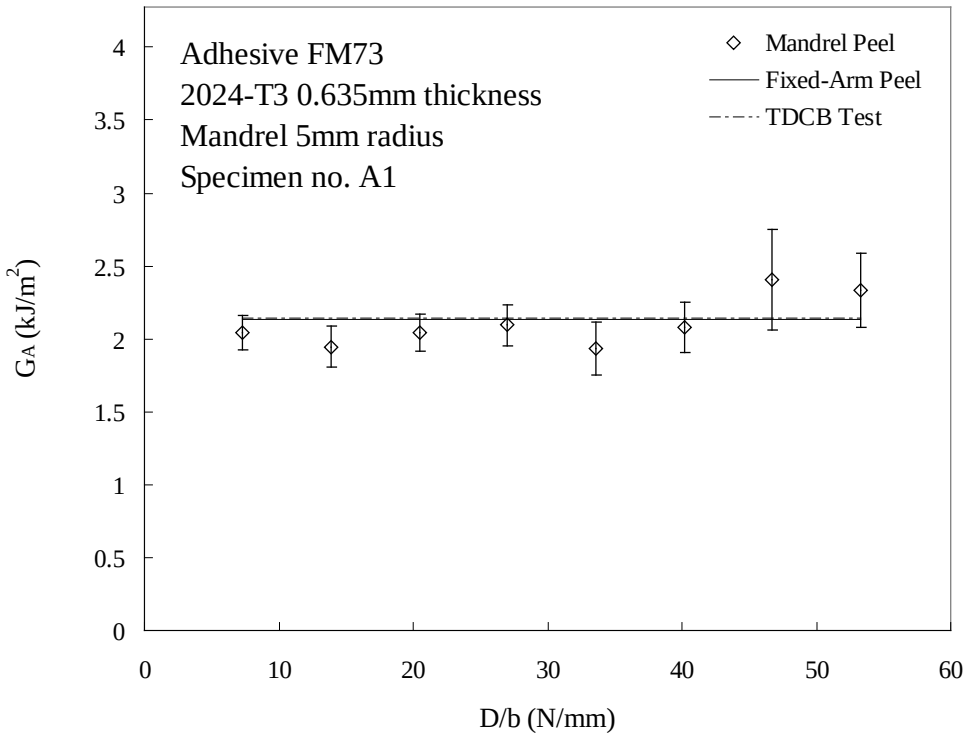

Figure 5 Peel results for 0.635 mm AA2024 T3/FM73 (specimen A1). Mandrel peel is conducted with a 5 mm radius roller and fixed arm peel relate to a 90^o peel angle. Fractures are cohesive.

The same test conditions were used for specimen A3 and results are shown in Figure 6 with *ICPeel* giving a value of radius of curvature of the peel arm of 11.5 mm. In this

case both mandrel and fixed arm peel generated interfacial fractures with associated lower values of G_A whilst the value of G_C from TDCB remains unchanged.
The radius of curvature of the peel arm (R_0 = 11.5 mm) is higher this time because the G_A for fixed arm peel is lower. Again there is a condition where $R_0 > R_1$ and as a consequence conformance of the peel arm can be expected. The independence of G_A with alignment load for the mandrel results again implies early conformance of the peel arm to the mandrel roller.
The values of G_A from fixed arm and mandrel peel show agreement; this is consistent with interfacial fracture in both tests. However, these values of G_A are about half the value for G_C from the TDCB test. The half value of G_C from TDCB has been shown to be approximately equal to interfacial fracture toughness at an interface [7].

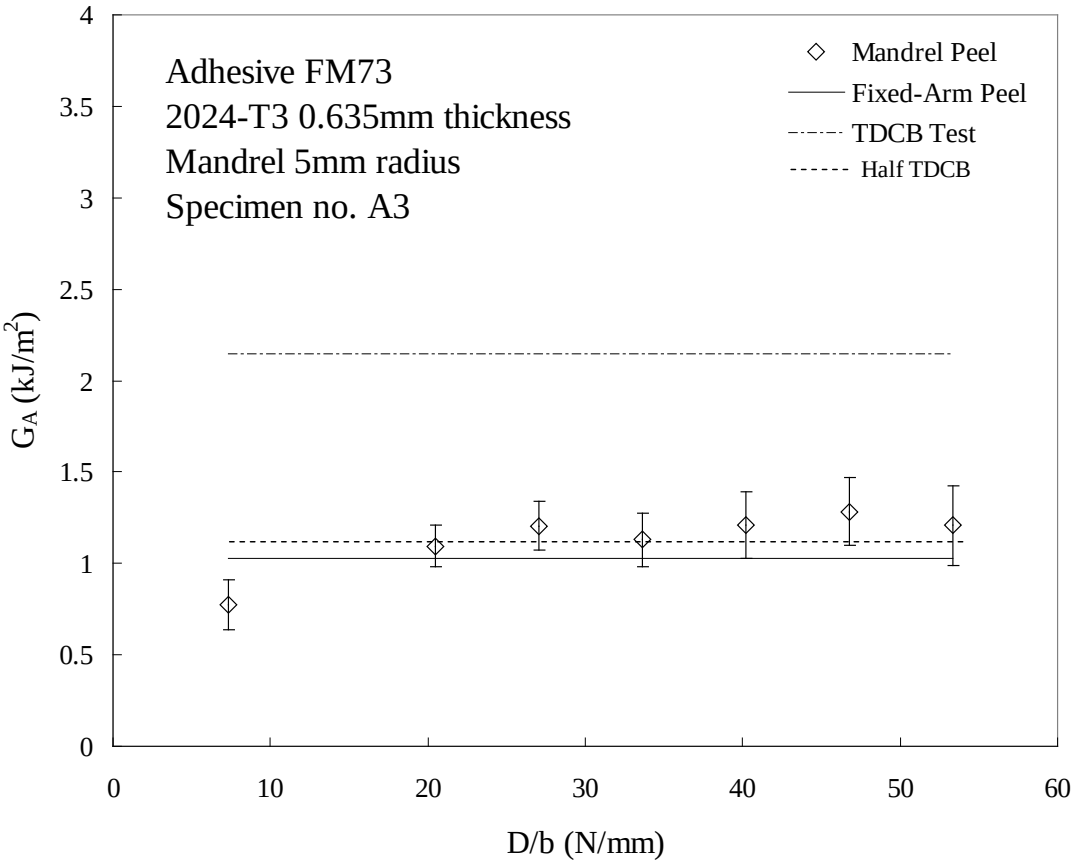

Figure 6 Peel results for 0.635 mm AA2024 T3/FM73 (specimen A3). Mandrel peel is conducted with a 5 mm radius roller and fixed arm peel relate to a 90^o peel angle. Fractures are interfacial for the peel tests and cohesive for TDCB.

The third specimen of 0.635 mm AA2024 T3/FM73 was tested with a mandrel roller radius of 7.5 mm using specimen number A2. Both fixed arm and mandrel peel generated interfacial fractures. Results are shown in Figure 7.
ICPeel provided a value of peel arm radius of curvature (R_0) of 10.9 mm for interfacial fracture. Therefore, there is a condition where R_0 is larger than R_1 and so conformance of the peel arm to the roller can be expected. However, with the use of a larger mandrel roller, conformance seems to occur at larger values of alignment load with higher values of G_A being observed at low alignment load. There is an

implication that data at low alignment loads might be cohesive before becoming interfacial since there is some adhesive coating on the photographs of the peel arm at low alignment load (see Figure 4) and the G_A value matches the cohesive fracture toughness from the TDCB test. However, the signs of cohesive fracture on Figure 4 are a result of the experimental set-up at the start of the peel process. At high alignment loads, where conformance of the peel to the mandrel roller has been achieved and where interfacial fracture occurs, the values of G_A from both peel tests are consistent with results from specimen A3. Again they are about half the value of cohesive fracture toughness from the TDCB test.

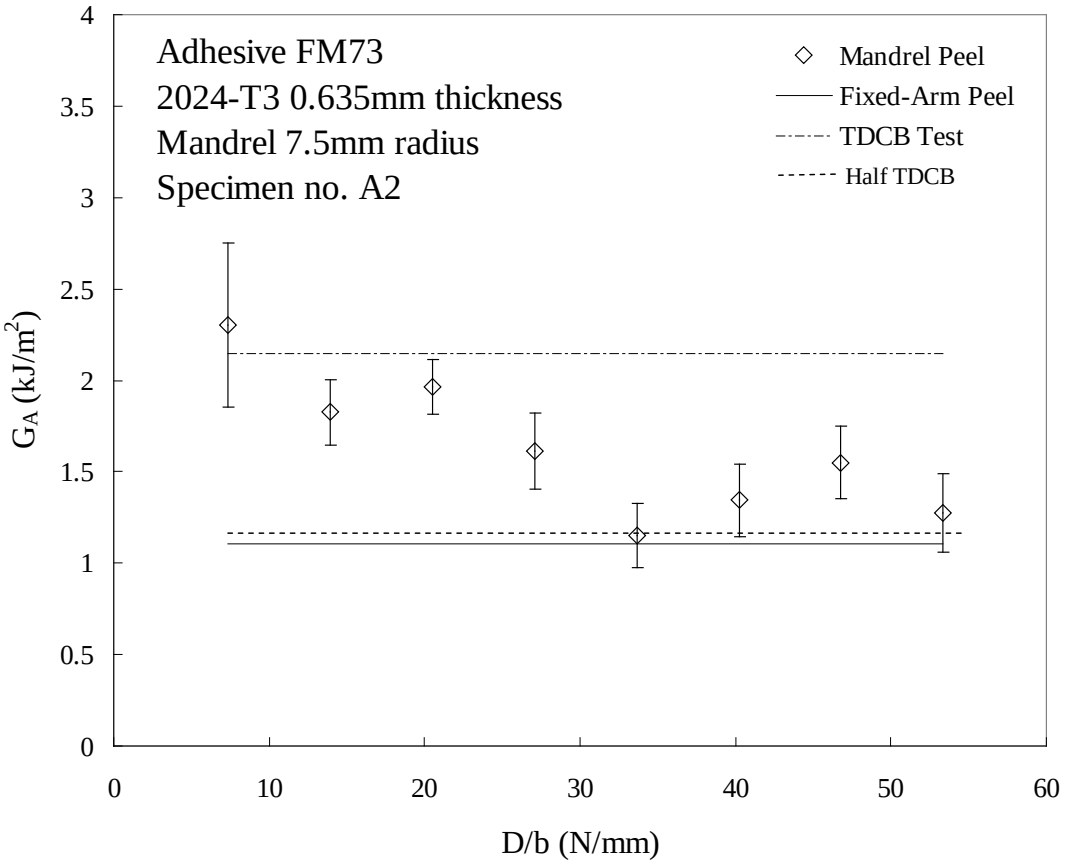

Figure 7 Peel results for 0.635 mm AA2024 T3/FM73 (specimen A2). Mandrel peel is conducted with a 7.5 mm radius roller and fixed arm peel relate to a 90^o peel angle. Peel fractures are interfacial.

In summary, the results for the 0.635 mm AA 2024 T3/FM73 laminate present two different forms of peel fracture but nevertheless the data sets are readily interpretable.

Results for laminate 0.635 mm AA2024 T3/Adhesive F.

A more comprehensive program of tests was conducted on specimens from the 0.635mm AA2024 T3/Adhesive F laminate. Fixed arm peel was based on multiple angle tests and mandrel peel used 5 different mandrel rollers of radii in the range 5 mm to 20 mm. In part, this is because a number of additional complications had to be accommodated.

Multi-angle fixed arm peel results are shown in Figure 8. As expected, both total external energy and plastic bending energy are peel angle dependent, but their

difference (adhesive fracture toughness) is independent of peel angle giving a mean value of 2560 J/m^2 with a standard deviation of 454 J/m^2.
The plane of fracture associated with these specimens exhibits asymmetric cohesive fracture. Optical micrographs of the peel arm surfaces are also shown in Figure 8. The diagonal crosshatch pattern is the textile binder associated with these film adhesives and for all specimens at the three peel angles there are visible remains of adhesive on the peel arms.

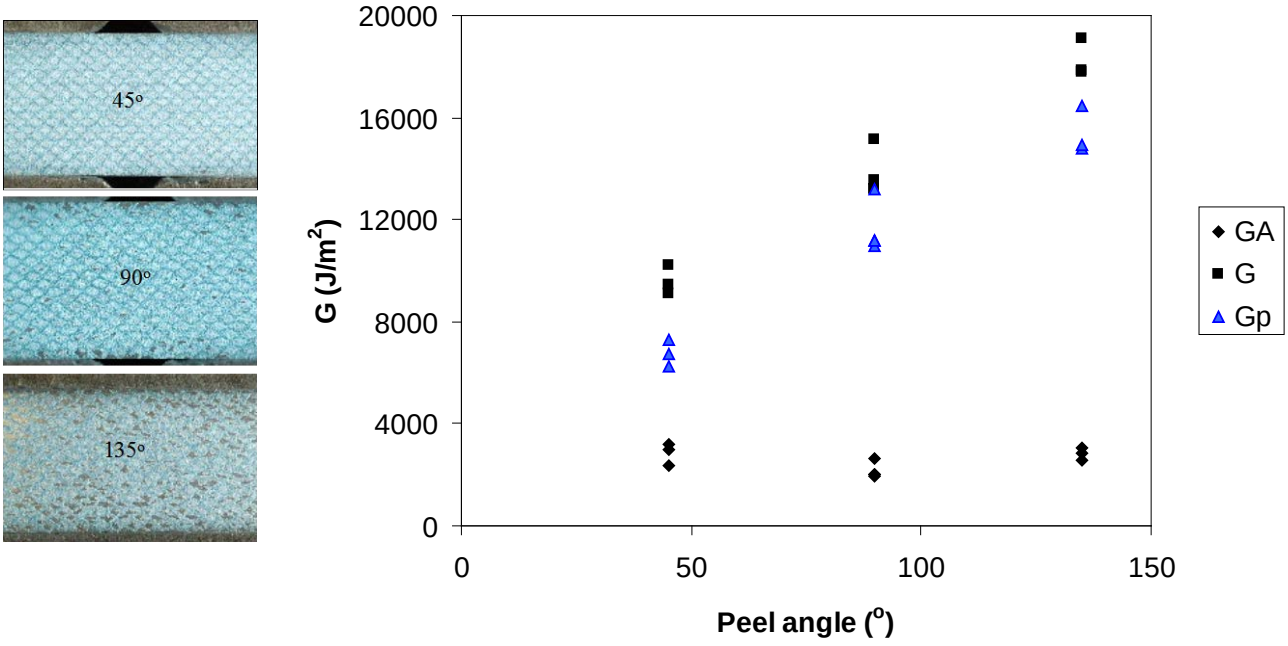

Figure 8 Fixed arm peel results for 0.635 mm AA 2024 T3/Adhesive F showing total external energy, plastic bending energy and adhesive fracture toughness. The micrographs show the fracture features on the peel arm surface.

Mandrel peel experiments were conducted with five different mandrel rollers, of radii (R_1) 5mm, 7.5mm, 10mm, 15mm and 20mm. A number of specimens were tested at each experimental set-up (usually up to five) in order to investigate reproducibility. Fixed arm data at a peel angle of 90^o enabled peel arm curvature at the crack tip (R_0) to be calculated (using *ICPeel* software); this gave a value of 6.0 mm. (This value agrees well with the measured value of peel arm radius at the crack tip by digital photography [12]). In order to achieve conformance of the peel arm to the mandrel roller it is necessary to apply an alignment load until $R_0 > R_1$. With R_0 = 6.0 mm it follows that this can never be achieved for roller radii of 7.5 mm to 20 mm, but can be achieved for the 5 mm roller radius.
Mandrel results for the 5 mm radius roller are shown in Figure 9 in the form of plots of G_A versus D/b. Five specimens have been tested using a range of alignment loads up to 100 kgs for 15 mm width (b) peel arms (D/b = 67 N/mm).
At low alignment loads, it would be expected that conformance of the peel arm to the roller might not fully occur (as shown in Figure 3 and observed for the 0.635 mm AA 2034 T3/FM73 laminate data with a roller radius of 7.5 mm), but as the alignment

load increases then conformance of the peel arm to the roller can be expected. The issue is therefore at what magnitude of alignment load does conformance occur i.e. at what value of *D/b* does $R_0 = R_1$. However, other issues are occurring as well as can be seen by inspection of the peel arms that provide interpretation of the plane of fracture.

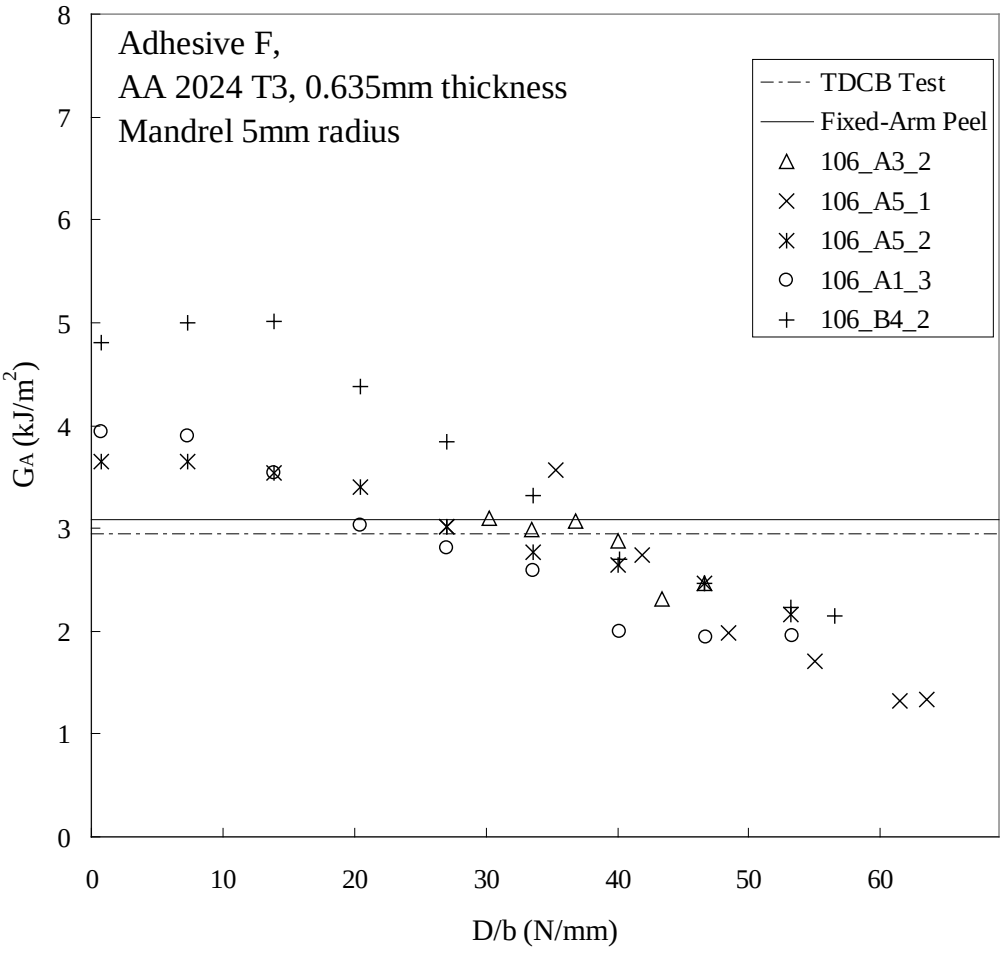

Figure 9 Mandrel peel data for 0.635mm AA 2034 T3/Adhesive F together with results from fixed arm peel and cohesive fracture toughness from TDCB test.

Optical micrographs of the peel arms from a selection of these mandrel specimens are shown in Figure 10, where the specimen numbers are the same as those used in Figure 9. A number of features can be seen:

(i) There is a transition from cohesive fracture to interfacial fracture as alignment load increases (specimen 106 A5 1). We have observed this type of fracture characteristic before [8] where it accounted for a fall in adhesive fracture toughness with alignment load, particularly at large alignment loads.

(ii) There are some specimens exhibiting cohesive fractures with an ample coating of adhesive on the peel arm (e.g specimen 106 B4 2) at all alignment loads.

(iii) There are peel arms where the surface appears partially interfacial at low alignment loads but cohesive at large alignment loads (specimen 106 A5

2). These show the smallest change in adhesive fracture toughness with increasing alignment load and it is believed that this effect is due to inconsistency in the specimen.

A full account as to why these affects occur is not possible, but it is likely that the surface treatment of the AA and the interaction between primer and adhesive will influence behaviour.

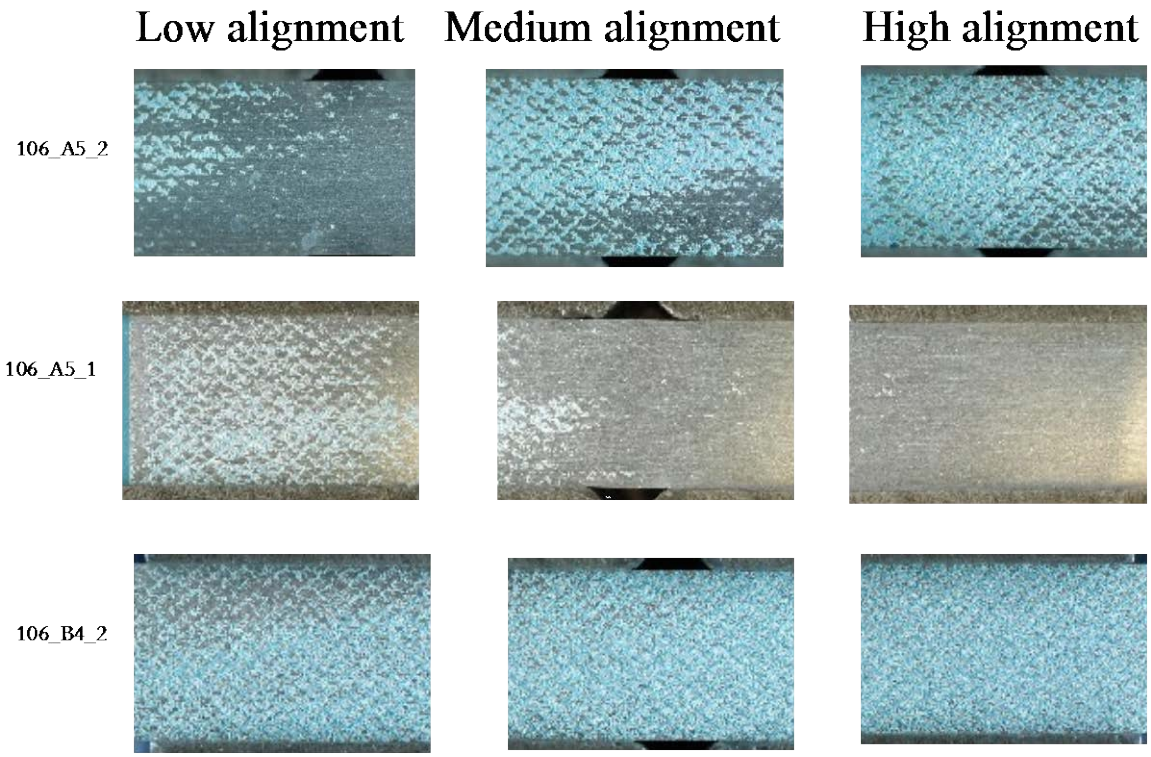

Figure 10 Optical micrographs of the peel surface for three specimens of 0.635 mm AA 2034 T3/Adhesive F tested with the mandrel equipment with a roller of radius 5 mm.

Overall, two effects can change the value of adhesive fracture toughness. First, non-conformance of the peel arm to the roller at low alignment loads, leading to a high initial value for G_A. However, as the alignment load increases so the value of G_A decreases to a steady value as conformance occurs. Second, a developing interfacial fracture with increasing alignment load, leading to a further reduction of G_A with alignment load. These effects will be superimposed and any specimen inconsistency will then further complicate observations.

With regard to the results in Figure 9 it can be seen that two extremes of behaviour occur at high alignment loads; fully cohesive fracture and fully interfacial fracture. Figure 11 shows the results for two specimens illustrating these extremes. The half value of the TDCB result is also included in this figure.

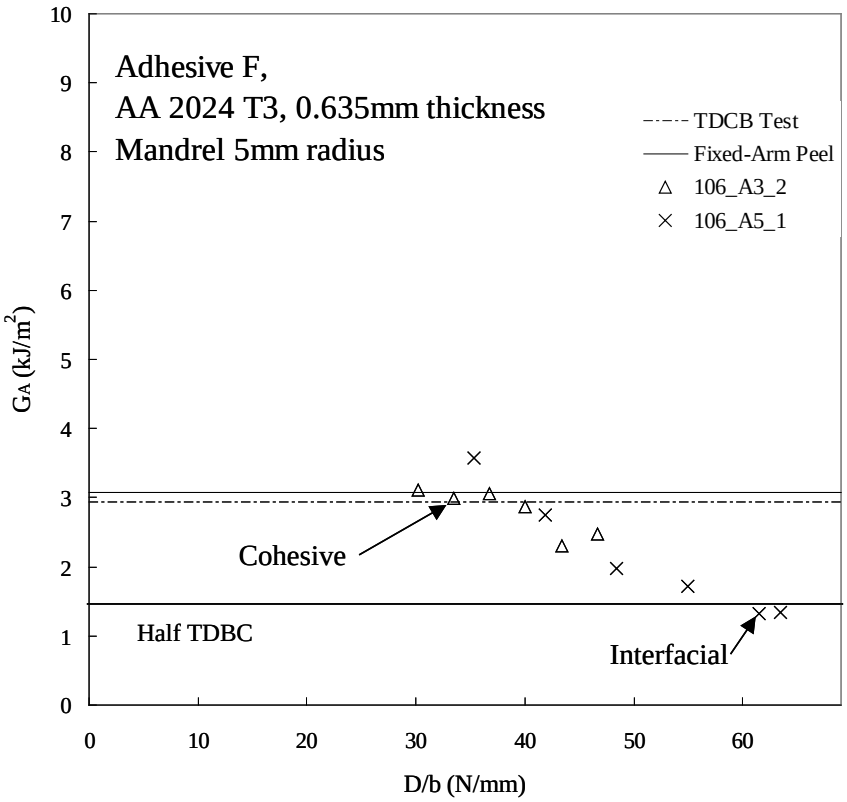

Figure 11 Plots of G_A versus D/b for 0.635 mm AA 2024 T3/Adhesive F from the mandrel apparatus with a 5 mm radius roller for cohesive and interfacial fractures.

The data relating to cohesive fracture are indicated in Figure 11. These results agree with the adhesive fracture toughness from fixed arm peel and also the G_C value from the TDCB test, both of which relate to cohesive fracture. The interfacial fracture data are also indicated on Figure 11 and these values agree with the half value from the TDCB test. This half value for G_C has been shown to approximate cohesive fracture toughness for fracture at an interface [7].

Overall, the results for the 5 mm mandrel roller radius are complex where a mixture of fracture planes can change the value of G_A. Nevertheless, there is good agreement between adhesive fracture toughness for cohesive fracture in the mandrel and fixed arm procedures and the values of G_A agree with the cohesive fracture toughness value (G_C) form the TDCB test. In addition, a value of interfacial adhesive fracture toughness is available from the mandrel method and this value agrees with an approximate G_C value at an interface.

Further consideration can be given to the confidence level associated with a value of G_A from the mandrel test in terms of the magnitude of the plastic bending correction. Equation 1 defines adhesive fracture toughness as the difference between total external energy and plastic bending energy. This can be considered in terms of a plastic bending energy correction (X) [10] and expressed as a percentage:

$$X = \{ \mathbf{100}(\frac{G_P}{G}) \} \qquad (5)$$

For the mandrel peel results, these corrections are shown in Table 1 together with the mean values of G_A for cohesive fracture.

Table 1 G_A, G_P and plastic corrections for 0.635 mm AA 2024 T3/Adhesive F from mandrel tests exhibiting cohesive fracture.

Mandrel roller radius (mm)	Mean G_A (J/m^2)	Measured G_P (J/m^2)	Plastic Correction (X) (%)
5	3000	12300	80
7.5	4660	7930	65
10	4660	4490	50
15	5650	2320	29
20	6870	1550	18

For the moment, only data relating to the 5 mm radius roller will be considered, where the plastic bending correction is given at 80%. Therefore, the separation between the bonded and the unbonded line is quite small for these mandrel tests. Inevitably, when seeking the difference between two large quantities (G and G_P in this case), then significant errors of measurement have to be accommodated. This merely adds to the dilemmas already discussed, whilst at the same time it makes the agreement between the cohesive toughness values even more striking.

Specimens from the 0.635 mm AA 2024 T3/Adhesive F laminate were also tested with the mandrel method with other roller sizes, namely roller radii (R_1) of 7.5mm, 10mm, 15 mm and 20mm. From what has already been presented, it can be expected that these specimens will never conform to the mandrel roller since in all cases $R_0 < R_1$, since R_0 is known to be 6 mm. However, all aspects of specimen inconsistency and transitions from cohesive to interfacial adhesion did not occur in any of the additional nine specimens that were tested. Indeed, some of these specimens were from the same plate of laminate that provided specimens for the 5 mm roller radius tests. All specimens exhibited a cohesive plane of fracture as shown for a selection of peel arm micrographs shown in Figure 12. Therefore, it seems apparent that the transitions from cohesive fracture to interfacial fracture for the tests conducted with the 5 mm radius roller are associated with high local stresses at the interface when the peel arm is conforming to the roller. It is also possible that subtle surface characteristics on the substrate are contributing as well (e.g. primer formulation, primer thickness, surface treatment of AA etc).

The mandrel results for the tests with roller radius between 7.5 mm and 20 mm are shown in Figures 13-16. In order to ease interpretation, common axes are used for all plots. The cohesive fracture toughness (from TDCB) and the adhesive fracture toughness from fixed arm peel tests are also shown in these figures. All fractures are cohesive.

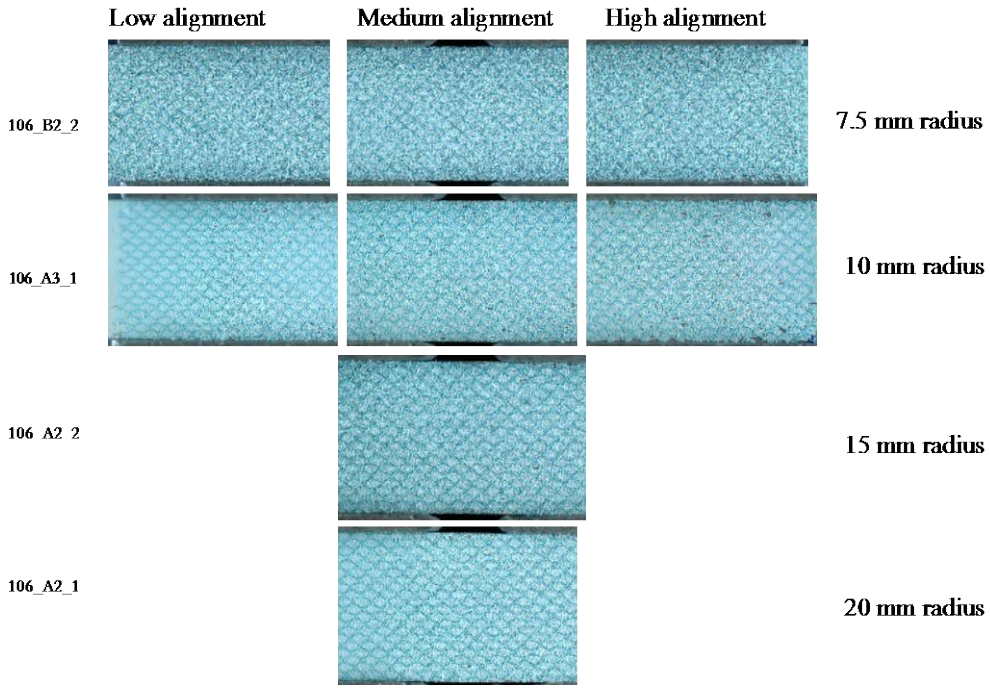

Figure 12 Optical micrographs of peel arms from 0.635 mm AA 2034 T3/Adhesive F laminate after mandrel testing with different mandrel roller radii.

Although none of these results relate to the peel arm conforming to the mandrel roller, the tests with the 7.5 mm radius roller are closest to conforming since in this case R_0 (6mm) is nearest to R_1 (7.5mm). Consequently, the data in Figure 13 approach the value of cohesive fracture toughness more closely than those for the data with the higher values of mandrel roller radius.

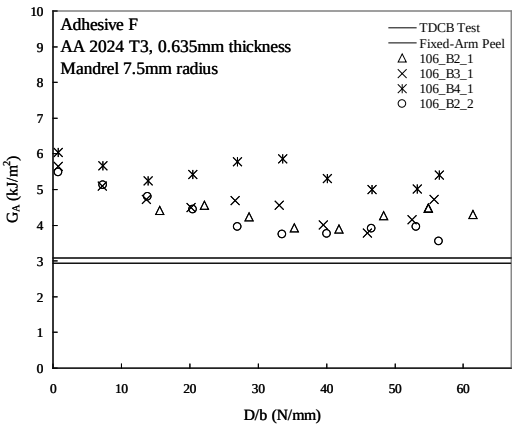

Figure 13 Mandrel results with roller radius 7.5 mm

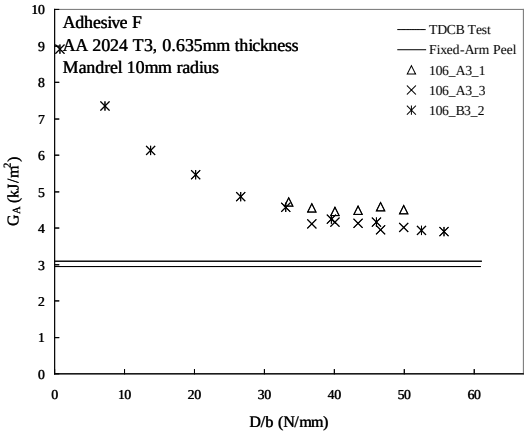

Figure 14 Mandrel results with roller radius 10 mm

Table 1 shows the mean values of adhesive fracture toughness determined from the data with the various roller radii. Values of G_A are obtained by analysis of plots of P/b versus D/b on the criterion that the slope of the line through the data for the bonded specimen is the same as that for the data for the unbonded specimens. Mean values of G_A are then calculated. It is apparent from the results in Table 1 that G_A increases as the degree of non-conformance increases, i.e. as the ratio R_0/R_1 decreases. It can also be seen from Table 1 that there is a reduction in G_P as the roller radius gets smaller. However, this is not a feature of non-conformance, as will be discussed later.

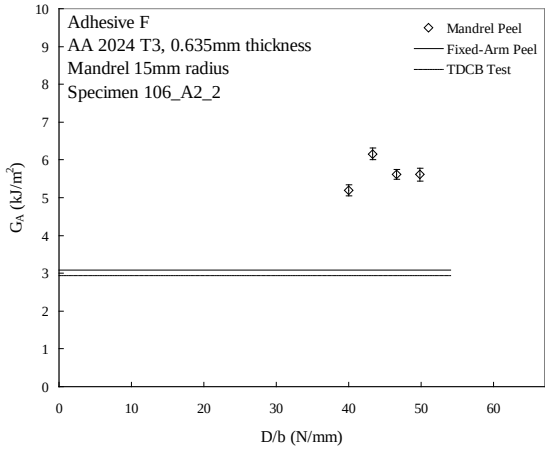

Figure 15 Mandrel results with roller radius 15 mm

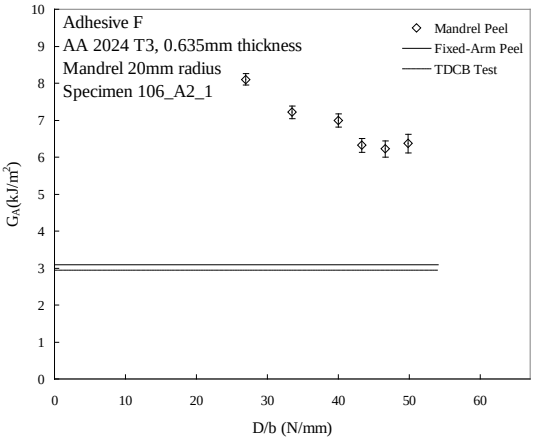

Figure 16 Mandrel results with roller radius 20 mm

Therefore, the greater the non-coformance of the peel arm to the mandrel roller, the larger the error in the value of G_A. This has also been observed in other roller assisted tests [8] and is indicative of the importance in being able to select an appropriate size of roller.

Table 1 shows the plastic bending energy correction as a function of mandrel roller radius. These are largest at small roller size and therefore the largest errors for G_A associated with this can be expected at smaller roller radii. A consideration of consequences that arise due to a large plastic bending energy correction (particularly for the data obtained with a 5 mm radius roller) can be investigated in part by a comparison of the measured value of G_P with the calculated value of G_P. The measured value is obtained from the mandrel peel test on the unbonded laminate. The calculated value is obtained from *ICPeel*, where Appendix 1 describes the calculations and includes the parameters obtained from the bilinear curve fitting of the stress-strain measurements on the peel arm. Results are shown in Figure 17.

The dashed line in Figure 17 is a linear fit with unit slope i.e. based on the measured and calculated values being identical. The thick continuous line is from a linear regression analysis of the data. It is seen that these lines are nearly identical giving confidence to the accuracy of the mandrel measurement with the unbonded laminates. This does not remove the difficulties in the determination of G_A associated with subtracting two large numbers (G and G_P) but it does lend some credibility to an achievement of best accuracy for the mandrel peel results.

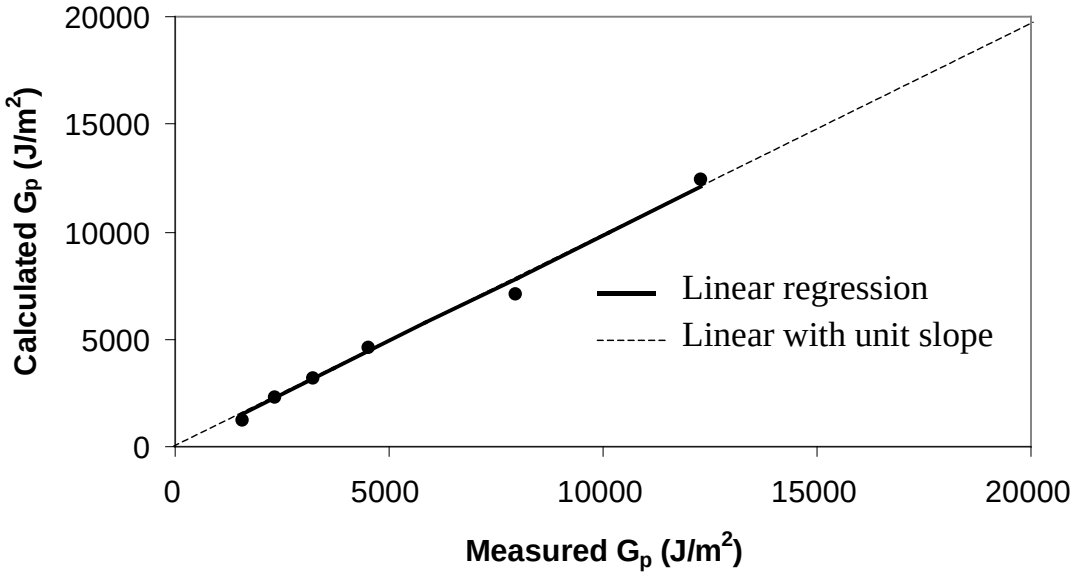

Figure 17 Calculated versus measured values of plastic bending energy for 0.635 mm AA 2024 T3/Adhesive F.

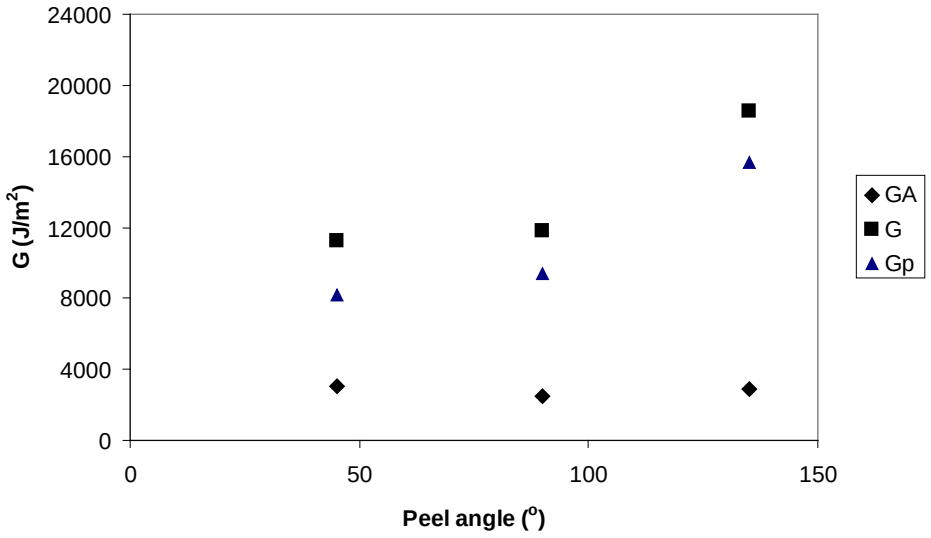

Figure 18 Fixed arm peel results for 1.635 mm AA 2024 T3/Adhesive F

Results for laminates 1.63 mm and 2.0 mm AA 2024 T3/Adhesive F

Experiments with laminates with thicker peel arms were conducted in order to investigate peel tests where much larger absolute values of plastic bending energy are involved. The mandrel tests were conducted with only one roller size (R_1 = 20 mm) chosen with an expectation of conformance of the peel arm to the mandrel roller. Results for the laminate with a peel arm of 1.635 mm are presented first. The variable angle fixed arm data are shown in Figure 18 where an average value of 2810 J/m^2 is

obtained for G_A that is independent of peel angle. Using the *ICPeel* software a value of R_0 of 29.6 mm is obtained for the radius of curvature of the peel arm at a peel angle of 90°. Consequently, the selection of a roller radius R_1 of 20 mm should enable conformance of the peel arm to be achieved during the mandrel peel tests, because $R_0 > R_1$.

Mandrel peel results on eight specimens are shown in Figure 19 together with cohesive fracture toughness from a TDCB test and G_A from the average of the fixed arm tests. All tests (for all conditions) exhibited a plane of fracture that was fully cohesive. Therefore a single plane of fracture is observed for these laminates.

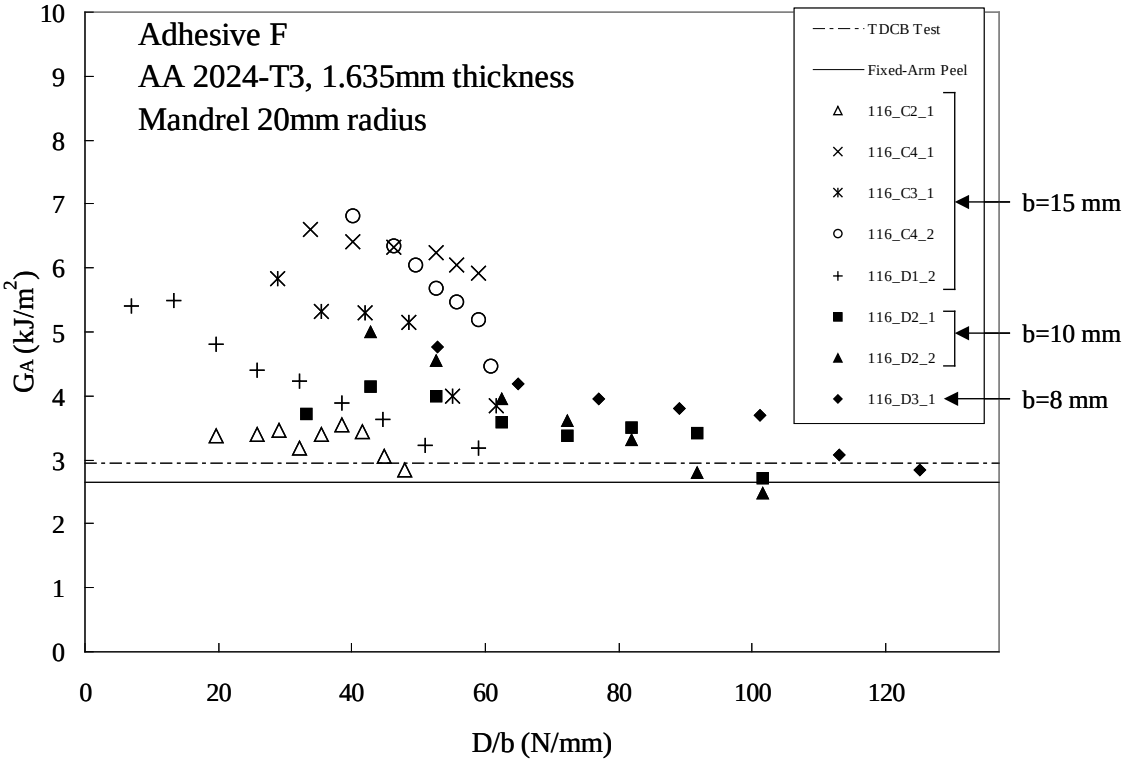

Figure 19 Mandrel results for 1.635 mm AA 2024 T3/Adhesive F with a 20 mm roller radius.

Two sets of mandrel experiments were conducted with the 1.635 mm peel arm laminates. The first set used our standard size for specimen width, namely b = 15 mm. Therefore with an alignment load of 100 kgs this achieved a D/b value up to about 60 N/mm. (These data are shown as unfilled characters in Figure 19). A second set of tests were also conducted where the width of the peel arm was smaller with b = 10 mm and b =8 mm. Therefore, with alignment loads up to 100 kgs, it was then possible to achieve D/b values up to 120 N/mm. (These data are shown as filled characters in Figure 19). With reference to results in Figure 19, it would be expected that at low values of alignment load there might be some non-conformance of the peel arm to the mandrel roller, but that as the alignment load is increased that conformance to the roller should be achieved. Therefore, G_A values at high alignment loads should show agreement between the mandrel data, the TDCB data and the fixed arm data. For the experiments with D/b values up to 60 N/mm, this is observed for perhaps four out of

the five specimens. Specimens 116 C2 1, 116 D1 2 and 116 C3 1 show agreement between G_A from mandrel and fixed arm methods and also show agreement with G_C from TDCB. Specimen 116 C4 2 suggests agreement at the highest alignment load, but specimen 116 C4 1 shows higher values of G_A.
It was speculated that amongst other reasons, a higher alignment load might rectify this problem and hence a second set of specimens were tested at higher alignment load (D/b) by reducing the peel arm width. Indeed these specimens (116 D2 1, 116 D2 2, 116 D3 1) then showed agreement between G_A at high alignment load and the adhesive fracture toughness from fixed arm peel and with the G_C value from TDCB test.

A similar approach was used with the laminate with the 2.0 mm peel arm. Figure 20 shows the variable angle fixed arm peel results where a mean value of 2924 J/m^2 is obtained for G_A. This is independent of peel angle and all fractures were fully cohesive. A value of R_0 of 41 mm is obtained from the *ICPeel* calculations on the 90^o fixed arm results. Therefore a mandrel procedure with a roller radius R_1 of 20 mm should ensure a condition for conformance of the peel arm i.e. where $R_0 > R_1$.

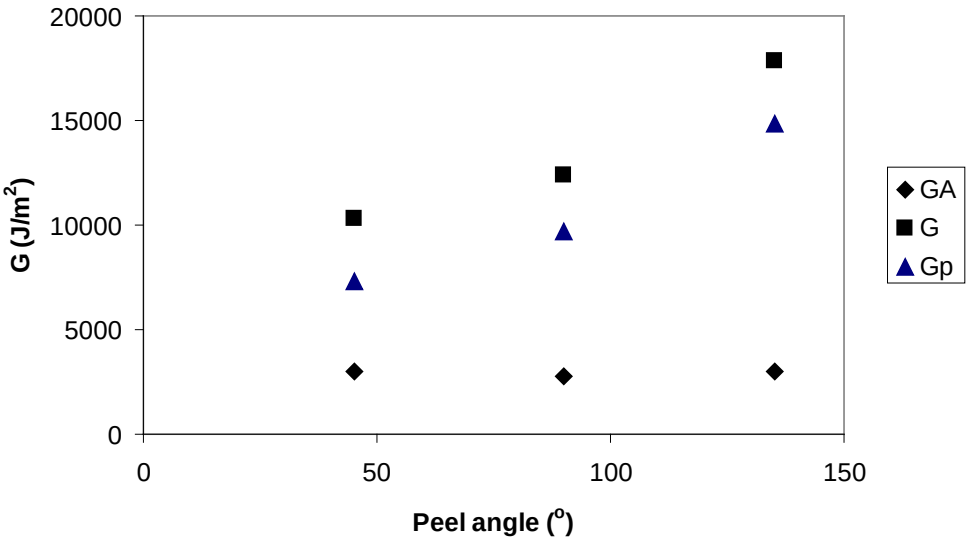

Figure 20 variable angle fixed arm peel for laminate 2.0 mm AA 2024 T3/Adhesive F

Figure 21 shows the mandrel data plotted with the TDCB results and average G_A from the fixed arm measurements. Again, two values of peel arm width were used. The data for standard width specimens (b = 15 mm) are shown with unfilled characters, whilst the data for narrower peel arms (b = 10 mm) are shown as filled characters and marked “narrow”). With alignment loads up to 100 kgs this enabled D/b values of up to 60 N/mm and up to about 100 N/mm, respectively. In general, all fractures were cohesive although the narrow peel arm specimens exhibited an interfacial edge effect. For the three standard width peel arms (b = 15 mm) and where alignment conditions reached 60 N/mm one showed the expected behaviour (specimen 120 E2 1) in that at high alignment loads the G_A from the mandrel test agreed with the toughness from TDCB and fixed arm peel. Another specimen (120 E3 2) gave the impression that at

higher alignment loads that the data might converge to agreement. However, specimen 120 E3 1 gave no signs of convergence of the data.
For the other three specimens where peel arm width was smaller (b = 10 mm) and the alignment conditions achieved values of D/b up to 100 N/mm, it was observed that the G_A values converged on the values of G_A from fixed arm peel. However, the G_A values from the mandrel test then became even lower with the highest values of D/b. It is possible that the interfacial edge effect observed with the narrow thick specimen could be responsible for this. Although, tests with thicker peel arms lead to other sources of possible errors as will now be discussed.

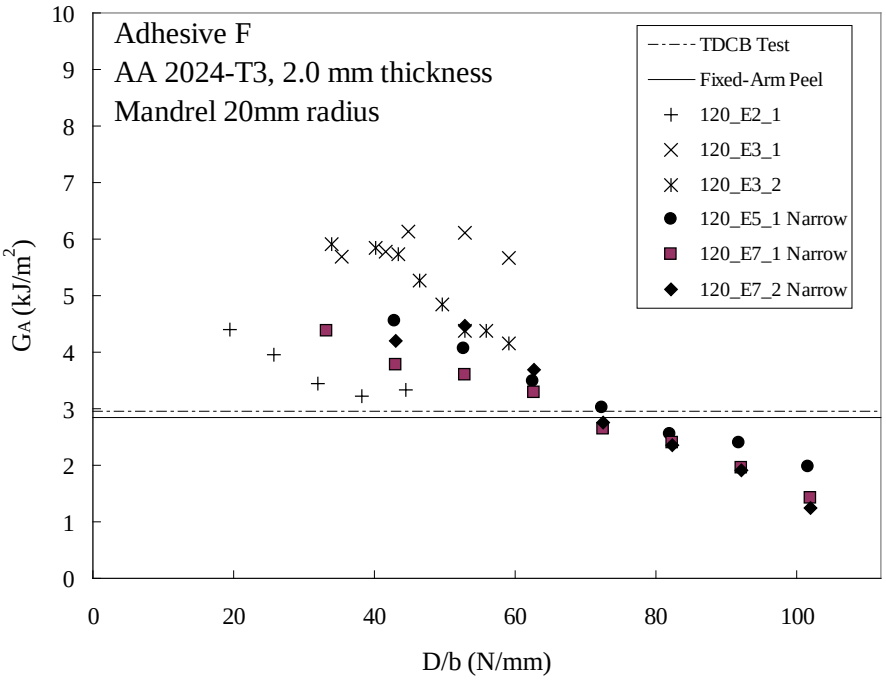

Figure 21 Mandrel results for 2.0 mm AA 2034 T3/adhesive F plotted with TDCB and the average of the fixed arm data.

A thicker peel arm will exhibit more plastic bending energy (all other considerations being equal) and therefore require more total external energy to achieve conformance to the mandrel roller. The magnitude of the plastic bending energy correction is large for the thicker peel arms. For the peel arm of thickness 1.635 mm X = 86% (on average) and for the 2.0 mm peel arm X = 78% (on average). Although these are values, they are similar to those for the earlier results with the 5 mm roller, where we also concluded confidence in the mandrel data.
For the results with thinner peel arms, it was helpful to consider a comparison of measured versus calculated plastic bending energy. This can also be done for the thicker peel arm laminates using the method previously described and detailed in Appendix 1.

Figure 22 shows calculated plastic bending energy (from *ICPeel* and Appendix 1) plotted against measured plastic bending energy (from unbonded mandrel peel). The results for the 0.635 mm laminates were discussed earlier. The line in Figure 22 is that of unit slope i.e. assuming that the two energies per unit area are equal. It is apparent

that the data for the 1.635 mm and 2.0 mm peel arms do not fit the unit slope line. In fact, $(G_P)_{CALCULATED} > (G_P)_{MEASURED}$. Therefore, if this can occur in some tests then the measured plastic bending energy will be too small and consequently the G_A value will be too large. The difference between measured and calculated values is of the order of 2000 J/m^2 and therefore this might constitute a possible error with the tests conducted on thick peel arms. However, the use of large alignment loads by reducing peel arm width seems to help in achieving good accuracy provided that there is an absence of an interfacial edge effect.

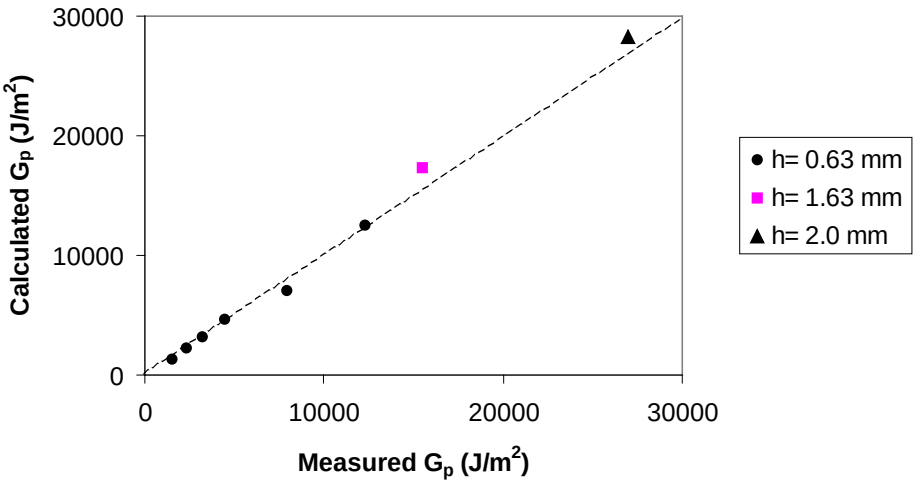

Figure 22 Calculated plastic bending energy versus measured plastic bending energy for all laminates.

CONCLUDING COMMENTS

The aim of this work was to conduct a systematic investigation of a mandrel peel test for measuring adhesive fracture toughness. It was also an aim to make comparisons of adhesive fracture toughness from mandrel peel with that from fixed arm peel and in addition to compare these toughness values with that from a cohesive fracture toughness method (TDCB). Two aerospace adhesive systems were used to facilitate this investigation with all the various idiosyncrasies associated with choice of substrate and surface treatment of this substrate.

In the mandrel peel test, our principle theme was to vary adherend thickness (peel arms of thickness 0.635mm, 1.635mm and 2.0 mm were used) and mandrel roller radius (five different sizes between 5 mm and 20 mm). For standard aerospace laminates, with a peel arm of 0.635mm, it was possible to observe cohesive and interfacial peel fractures. The adhesive fracture toughness for cohesive fracture was larger than that for interfacial fracture and when there was a transition from cohesive to interfacial fracture during the peel test, this phenomenon complicated the toughness measurement procedures. Transitions in the plane of fracture occurred for both mandrel and fixed arm peel but did not necessarily occur every time. In the TDCB test only cohesive fractures were exhibited. However, when all methods exhibited cohesive fracture, there was generally good agreement in toughness.

A method was developed for mandrel peel with predictability of conformance of the peel arm to the mandrel roller (or not as the case maybe). It has been established that the radius of curvature of the peel arm (R_0) had to be larger than the mandrel roller

radius (R_1) in order to achieve peel arm conformance with increasing alignment load. The value of R_0 could be determined from a fixed arm peel method in order to predict what mandrel roller size would enable peel arm conformance. Mandrel results with a range of roller sizes established this methodology.

The methods were further investigated with non-standard aerospace laminates where the peel arm thickness was larger at values of 1.635 mm and 2.0 mm. Tests were conducted using mandrel rollers where conformance of the peel arms to the mandrel were expected. In general, there was agreement between G_A form mandrel and fixed arm peel and with toughness from TDCB.

There were some difficulties associated with the mandrel tests with thick peel arms. In general, the root cause of these problems seemed to be associated with a high plastic bending energy (in absolute terms) for the thick peel arm laminates. Extremely high alignment loads could accommodate these issues provided that interfacial edge effects were not experienced. Consequently, there seems to be no benefit in altering the standard aerospace laminate (with its 0.635 mm peel arm) used for peel tests.

The overall content of this work enables a protocol for a mandrel peel method to be established. It is believed that the mandrel peel method can usefully complement existing peel procedures for metal polymer laminates.

ACKNOWLEDGEMENTS

The authors acknowledge support from the Royal Academy of Engineering, Cytec Engineered Materials and ICI plc for D R Moore and support from IMRE, Singapore for L F Kawashita.

REFERENCES

[1] ASTM D 1781-93, *Standard Test Method for Climbing Drum peel for Adhesives* (1993).

[2] ASTM D 3167-97, *Standard Test Method for Floating Roller Peel Resistance of Adhesives* (1997).

[3] D. R. Moore, A. Pavan, J.G.Williams, eds *Fracture Mechanics Testing Methods for Polymers, Adhesives and Composites*, B. Blackman, A.J. Kinloch, Ch 3 p 225 *Fracture Tests on Structural Adhesive Joints* ISBN 008 0436897 Elsevier, Oxford, 2001

[4] D R Moore ed *The Application of Fracture Mechanics to Polymers, Adhesives and Composites* ISBN 0080442056 Elsevier, Oxford, 2004

[5] D. R. Moore, A. Pavan, J.G.Williams, eds *Fracture Mechanics Testing Methods for Polymers, Adhesives and Composites*, J.G. Williams *Introduction to Linear Elastic Fracture Mechanics*, p 3 ISBN 008 0436897 Elsevier, Oxford, 2001

[6] A.J. Kinloch, C.C. Lau, and J G Williams, *Int. J. Fract.*, **66**, 45-70 (1994).

[7] L F Kawashita, D R Moore, J G Williams, *The Measurement of Cohesive and Interfacial Toughness for Bonded Metal Joints with Epoxy Adhesives* pending publication in *Composite Interfaces* (2005).

[8] L F Kawashita, D R Moore, J G Williams, *J Adhesion*, 81, 561, (2005)

[9] I. Georgiou, H. Hadavina, A. Ivankovic, A.J. Kinloch, V. Tropsa, J.G. Williams,. *The Journal of Adhesion*, 79, 1-27 (2003).

[10] D. R. Moore, A. Pavan, J.G.Williams eds *"Fracture Mechanics Testing Methods for Polymers, Adhesives and Composites*, D.R. Moore, and J.G. Williams, Ch 3 p 203 ISBN 008 0436897 Elsevier, Oxford, 2001.

[11] Imperial College website, http:/www.me.ic.ac.uk/AACgroup/ peel test protocols-ICPeel
[12] L. F. Kawashita, D. R. Moore, J. G. Williams *J. Mat. Sci.* 40, (2005) 1-8
[3]A, N. Gent, & S.Y. Kaang, *J Adhesion*, **24**, 173-181 (1987).
[4] E Breslauer, T. Trocynski, *J.Adhesion Sci. Technol.*, **12**,. 4 367-382 (1998).
[15] L F Kawashita, D R Moore, J G Williams, J.G., *The Journal of Adhesion*, 80, 1-21, (2004)

APPENDIX 1 CALCULATION OF PLASTIC BENDING ENERGY

The plastic bending energy is given by [6,9]:

$$G_P = \frac{E\varepsilon y^2 h}{2} f(k_0)$$

where k_0 is the maximum curvature of the adherent, E is an elastic modulus of the peel arm material, h is its thickness and ε_y is its yield strain. $f(k_0)$ is described fully in reference [9] and is dependent on the parameters of the stress-strain($\sigma-\varepsilon$) model and loading-unloading conditions. The tensile stress-strain behaviour of the peel arm has been measured and fitted to a bilinear function. Table A1 shows the parameters from the fit. The bilinear function is described as follows:

When $\varepsilon \le \varepsilon_y$,

$$\sigma = E\varepsilon$$

When $\varepsilon > \varepsilon_y$,

$$\sigma = \sigma_y + \alpha E(\varepsilon - \varepsilon_y)$$

Table A1 Tensile properties of AA 2024-T3 based on a bilinear fit to experimental data.

Elastic modulus (E) (GPa)	Plastic modulus (E_P) (GPa)	Work hardening coefficient (α) (E_P/E_1)	Yield strain (%)	Yield stress (MPa)
70	2.5	0.035	0.51	360

The maximum curvature is given by [9]:

$$k_0 = \frac{h}{2\varepsilon_y R_0}$$

where R_0 is the minimum radius of curvature. In a mandrel test, R_0 is obtained from the mandrel radius and the peel arm thickness, namely

$$R_0 = R_1 + \frac{h}{2}$$

There are three cases to consider in the determination of the $f(k_0)$ functions:

Case 1: Elastic bending and unbending

$0 < k_0 \leq 1$

then

$$f\left(k_0\right) = 0$$

Case 2: Plastic bending and elastic unbending

$$1 < k_0 \leq 2\frac{(1-\alpha)}{(1-2\alpha)}$$

then

$$f\left(k_0\right) = (1-\alpha)\left[\frac{1}{3}k_0{}^2 + \frac{2}{3k_0} - 1\right]$$

Case 3: Plastic bending and unbending

$$k_0 > 2\frac{(1-\alpha)}{(1-2\alpha)}$$

then

$$f(k_0) = \frac{4}{3}\alpha[(1-\alpha)(1-\frac{\alpha}{2}) - \frac{1}{8}]k_0{}^2 + 2(1-\alpha)(1-\frac{\alpha}{2})(1-2\alpha)k_0 + \frac{2(1-\alpha)}{3(1-2\alpha)k_0}\beta - (1-\alpha)\gamma$$

where

$$\beta = [1 - 2\alpha^2(2-\alpha) + 4(1-\alpha)^3]$$

and

$$\gamma = [1 + 2\alpha(1-\alpha) + 4(1-\alpha)^2]$$

In practice, case 3 is the most common and applies in this work.
The *ICPeel* [11] software accommodates these functions in order to calculate the plastic bending energy.